On-Surface Synthesis of Hydrogen-Substituted γ-Graphdiyne with High Efficiency
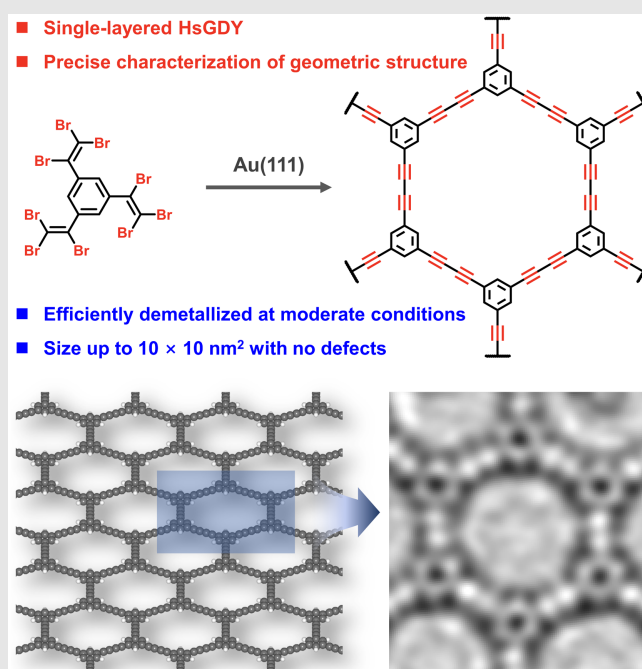
Faming Kang[1†], Wei Zheng[1†], Luye Sun[1], Wenze Gao[1], Lina Shang[1], Lifeng Chi[2*] & Wei Xu[1*]

[1]Interdisciplinary Materials Research Center, School of Materials Science and Engineering, Tongji University, Shanghai 201804, [2]Institute of Functional Nano & Soft Materials (FUNSOM), Jiangsu Key Laboratory for Carbon-Based Functional Materials and Devices, Joint International Research Laboratory of Carbon-Based Functional Materials and Devices, Soochow University, Suzhou 215123

*Corresponding authors: xuwei@tongji.edu.cn; chilf@suda.edu.cn; †F. Kang and W. Zheng contributed equally to this work.

Graphyne, a remarkable two-dimensional carbon allotrope, has attracted significant attention in the field of materials science due to its unique properties and potential applications. Because of the special arrangement of their sp- and sp²-hybridized carbon atoms, these structures display a wide range of geometrical and electronic characteristics as well as homogeneous pores of varying sizes, making them suitable for a variety of practical applications. In recent years, the synthesis of the thin film products of graphyne and its derivatives has typically been documented. To date, however, it remains challenging to synthesize atomically precise single-layered graphyne and its derivatives. Herein, we report a facile strategy to synthesize single-layered hydrogen-substituted γ-graphdiyne on the Au(111) surface through dehalogenation and intermolecular coupling polymerization. Its geometric atomic structure was investigated by scanning probe microscopy. Combined with theoretical results, we reveal its semiconducting property.

- Single-layered HsGDY
- Precise characterization of geometric structure

Au(111)

- Efficiently demetallized at moderate conditions
- Size up to 10 × 10 nm² with no defects

Keywords: scanning probe microscopy, on-surface synthesis, γ-graphdiyne, hydrogen-substituted γ-graphdiyne, electronic structures

Introduction

Carbon-rich molecules and materials have been extensively studied for decades, fueled by the successive generations of novel carbon allotropes such as diamonds, fullerenes,[1] carbon nanotubes,[2] and graphene.[3] These carbon allotropes can yield surprising results both in terms of their mechanical strength and their possible

applications, such as in the next generation of electronics. The theoretical discovery of graphyne-family structures has opened up new avenues for the exploration and development of two-dimensional carbon materials.[4] Graphyne-family structures are a range of hybrid carbon allotropes composed of sp- and sp²-hybridized carbon atoms, possessing intriguing properties distinct from other carbon-based materials.[5-7] However, direct production of these kinds of materials is never easy. One member of the family, γ-graphdiyne (GDY) (Figure 1a), exhibits a honeycomb-like lattice structure, featuring interconnected benzene rings and acetylene units, resulting in a unique arrangement of carbon atoms. Since Li's pioneering work[8-10] on experimental preparation of a uniform GDY film via the Glaser coupling reaction in solution, several synthetic approaches have been developed to obtain high-quality GDY films. These methods include bottom-up synthesis,[11,12] top-down lithography techniques,[13] and chemical vapor deposition processes.[14] Each method offers advantages and challenges, and researchers continue to refine and optimize the synthesis techniques to achieve large-scale production of GDY. The research on graphdiyne has gained momentum in recent years, with numerous studies investigating its properties and exploring its applications.[15-17] However, the synthesis of single-layered GDY and its derivatives, such as hydrogen-substituted γ-graphdiyne (HsGDY) (Figure 1b), on a large scale, presents several challenges due to the complex and intricate nature of their structure and reactivity. Thus, developing efficient synthesis methods that can produce such single-layered structures with consistent quality is an ongoing research area.

On-surface synthesis is an emerging strategy for creating unique low-dimensional carbon nanostructures,[18] which has successfully added sp-hybridized carbon atoms to nanostructures in recent years. The acetylenic and cumulenic motifs have now been successfully created using dehalogenative homocoupling reactions.[19-23] One of these motifs, diacetylene (C≡C–C≡C), which is a typical motif in GDY and HsGDY, has already been produced by dehalogenative homocoupling of terminal alkynyl bromides on the Au(111) surface.[24] This has made on-surface synthesis of GDY and its derivatives an active research area and offers great potential for tailoring the properties of these structures on the atomic scale. We should point out that, in such an on-surface reaction process, the formation of organometallic intermediates (C≡C–M–C≡C) is usually inevitable,[24-26] and demetallization is a challenging process that normally hampers further formation of large-area and high-quality metal-free two-dimensional structures. Thus, the development of an on-surface synthesis strategy devoid of organometallic intermediates or, on the other hand, to efficiently promote the demetallization at moderate conditions is urgently needed.

Recently, chlorine atoms were found to be crucial in assisting the breakage of metal-alkynyl bonds.[27] Inspired by this work, we introduced a new functional group, tribromoethenyl, which is anticipated to undergo β-elimination and dehalogenative organometallic homocoupling reactions. More importantly, more bromine atoms were also introduced onto the surface, which was expected to facilitate the demetallization from the organometallic intermediates. Experimentally, we designed and synthesized two precursors with one and three tribromoethenyl groups to generate metal-free dimer and network (i.e., HsGDY) products. As expected, they were successfully produced under moderate conditions. The structure of the synthesized HsGDY network was unambiguously characterized by means of scanning tunneling microscopy (STM) and noncontact atomic
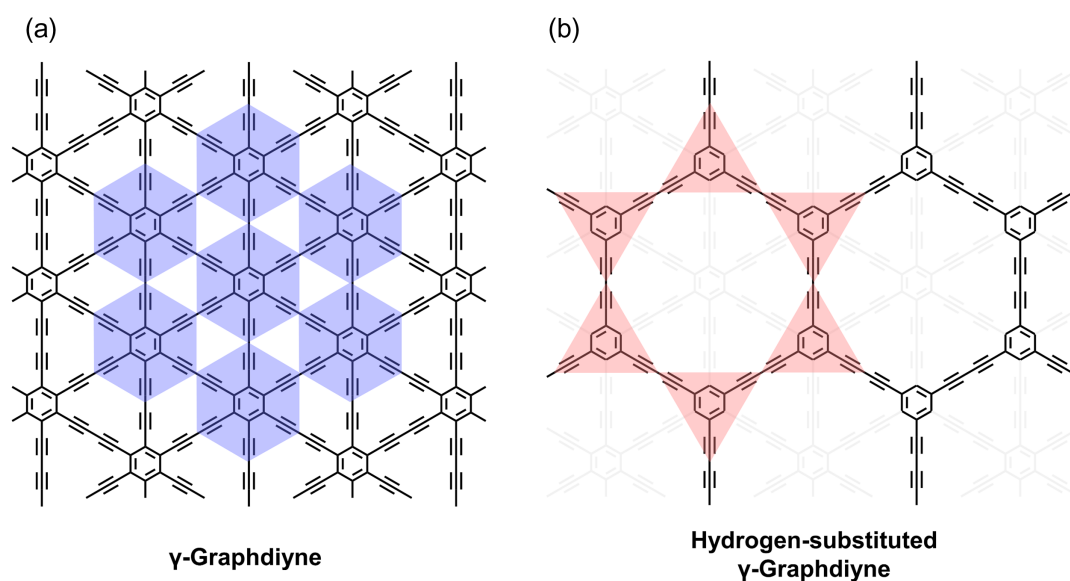

γ-Graphdiyne

**Hydrogen-substituted
γ-Graphdiyne**

Figure 1 | *Structures of (a) GDY and (b) HsGDY networks.*

force microscopy (AFM). The electronic structure and properties of the HsGDY network were investigated by density functional theory (DFT) calculations.

Results and Discussion

First, we tried to investigate the molecule with one tribromoethenyl group (4-(1,2,2-tribromoethenyl)-1,1′-biphenyl, TBEBP) and also compared it with another previously studied molecule with bromoalkynyl group (4-(bromoethynyl)-1,1′-biphenyl, BEBP) on the Au(111) surface. We found that both functional groups underwent dehalogenative organometallic coupling after deposition of molecules on Au(111) held at 300 K, resulting in the formation of organometallic intermediates, as shown in Figure 2a,b. Interestingly, a milder annealing condition (360 K vs 400 K) was required for the further
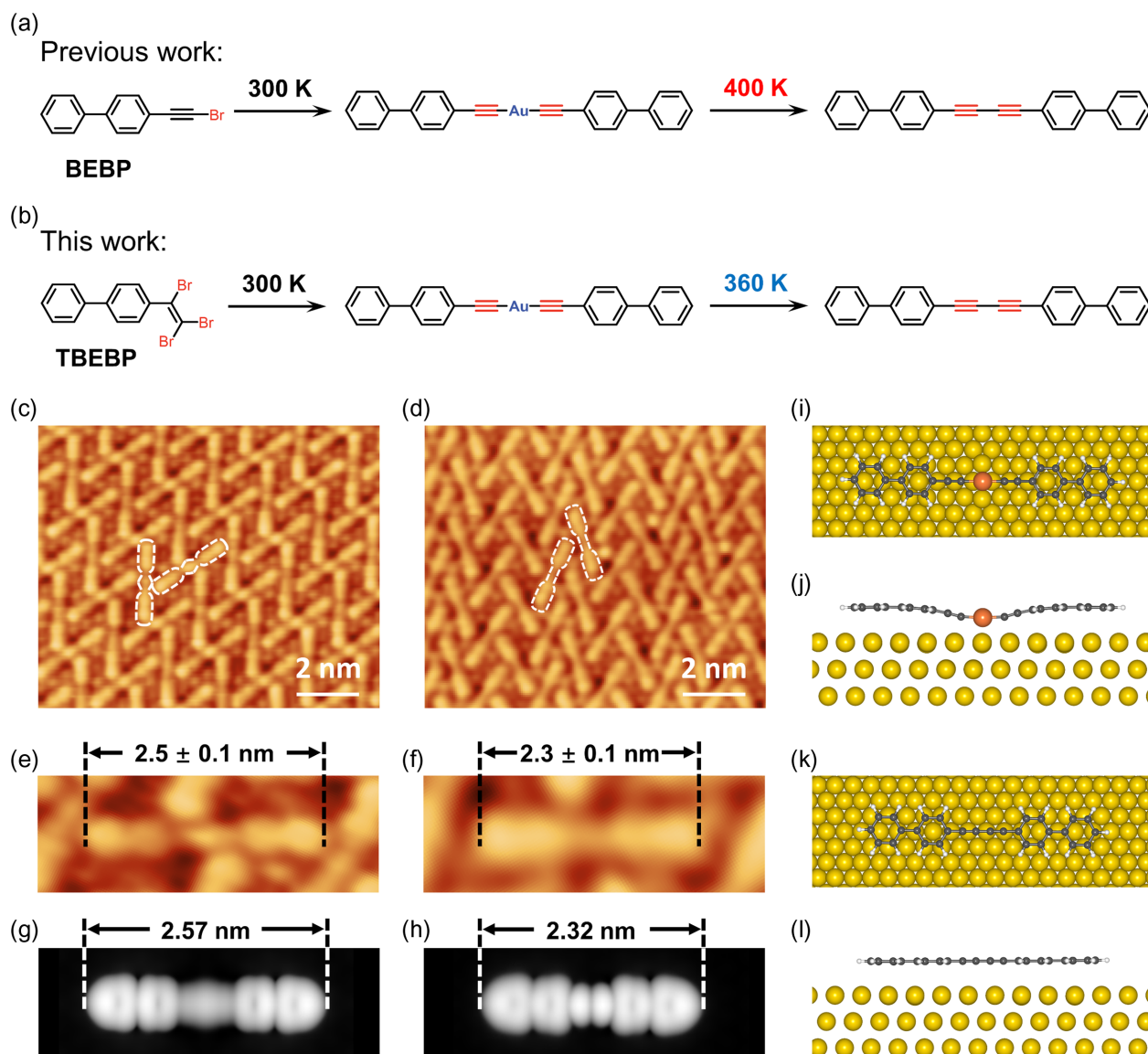

Figure 2 | *Comparison of on-surface reactions of molecular precursors with bromoalkynyl and tribromoethenyl groups on the Au(111) surface, respectively. Schematic illustrations showing the formation of the same organometallic intermediate and the metal-free dimer product originating from (a) BEBP and (b) TBEBP with different temperatures, respectively. Large-scale STM images of the samples (c) after deposition of TBEBP on Au(111) held at about 300 K and (d) after annealing at about 360 K. STM images of (e) organometallic intermediate and (f) metal-free dimer product. The corresponding DFT-calculated STM images are shown in (g) and (h). The calculated models of the organometallic intermediate are shown in (i) top view and (j) side view. Also, the calculated models of the dimer product are shown in (k) top view and (l) side view. Scanning parameters: STM images (c), V = −1.05 V, I_t = 0.79 nA, (d), V = −1.25 V, I_t = 0.69 nA, (e), V = −1.25 V, I_t = 0.71 nA, and (f), V = −1.05 V, I_t = 0.69 nA.*

demetallization process by using TBEBP molecules. The lower annealing temperature for the demetallization was attributed to the fact that there were more bromine atoms involved in this process.[27] The detailed experimental results are shown in Figure 2c–f, where STM images reveal the formation of the organometallic coupling intermediates and the demetallized products. The individual intermediates and the products are marked by the white contours, respectively, which are further illustrated in the close-up images and compared with the theoretical simulations (Figure 2g, h). The DFT-calculated models in the top and side views are demonstrated in Figure 2i–l.
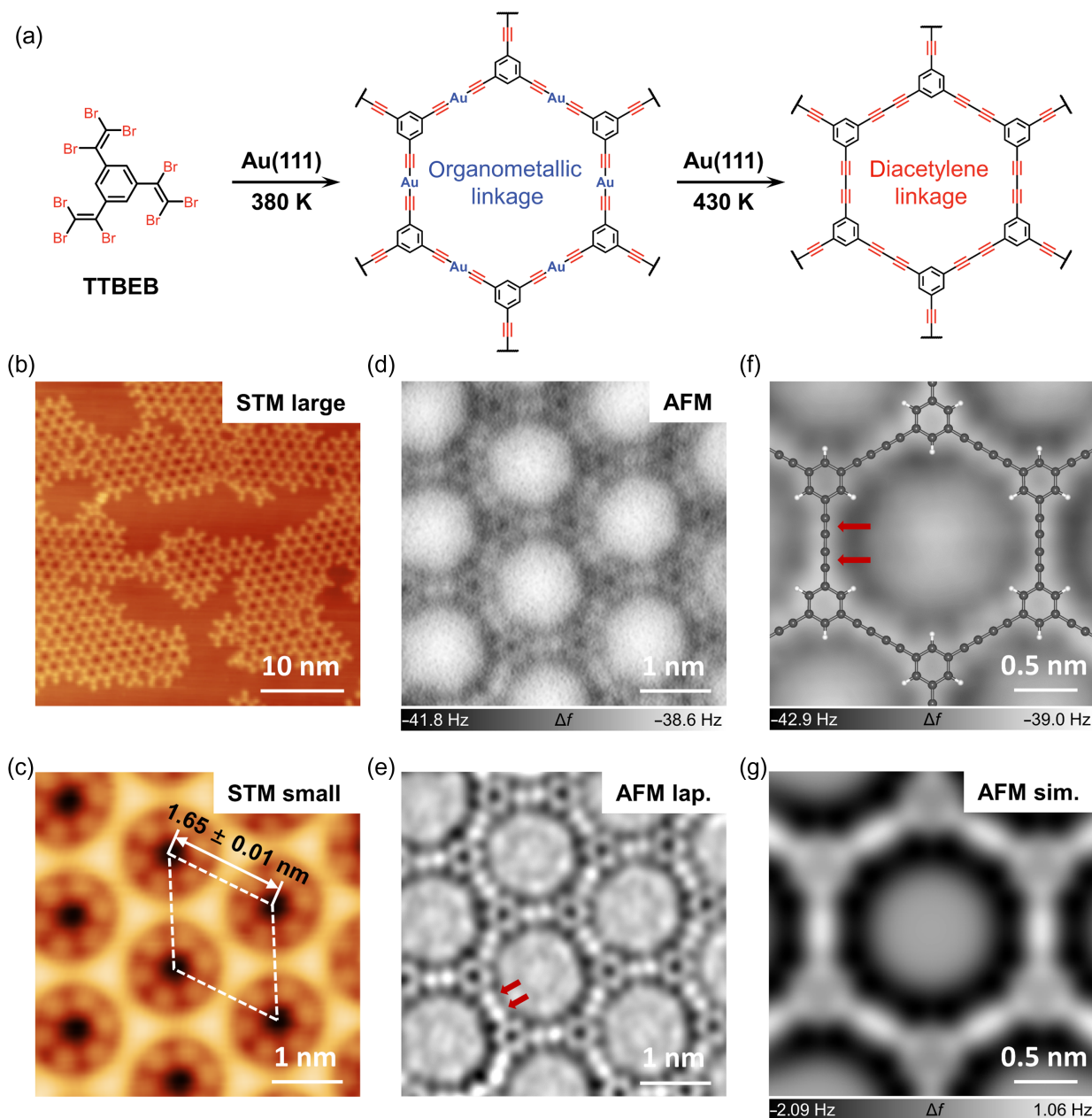

Figure 3 | *Synthesis and structural characterization of HsGDY on the Au(111) surface. (a) Synthetic strategy from TTBEB molecular precursor to HsGDY with high efficiency. (b) Large-scale STM image of HsGDY network obtained after deposition of TTBEB on Au(111) and further annealing the sample at 430 K. (c, d) Close-up STM and AFM images of HsGDY. (e) Corresponding Laplace-filtered AFM image. (f) AFM image of a hexagonal unit with relaxed structural model overlaid, and two red arrows indicating the diacetylene moiety. (g) Simulated AFM image based on DFT calculated gas-phase geometry. Scanning parameters: STM image (b), V = −0.88 V, I_t = 0.96 nA, (c), V = 0.30 V, I_t = 50 pA; all AFM images were recorded with a Br-tip at different tip offsets z, with respect to an STM set point, 0.30 V, 50 pA. (d: −80 pm, f: −70 pm).*

We then synthesized the 1,3,5-tris(1,2,2-tribromoethenyl)benzene (TTBEB) molecule with three tribromoethenyl groups with the aim of producing high-quality HsGDY networks. The organometallic network was obtained after deposition of TTBEB molecules on Au(111) held at about 300 K and slightly annealed at 380 K, as shown in Supporting Information Figure S1, also as reported previously.[24] After annealing the sample at 430 K, the metal-free HsGDY networks were subsequently produced, as illustrated in Figure 3a. Experimentally, we observed from a large-scale STM image (Figure 3b) that the HsGDY structures were distributed as islands on the surface. The close-up STM image allowed us to identify the metal-free HsGDY network structure as shown in Figure 3c. More detailed structural information can be seen in the corresponding AFM images (Figure 3d,e), in which the diacetylene moiety was imaged as two characteristic bright protrusions[28-31] (indicated by two red arrows in Figure 3e) can be unambiguously distinguished. The relaxed model matched well with the AFM

image (Figure 3f), and the corresponding AFM simulation is also shown in Figure 3g. In comparison with our previous work employing the bromoalkynyl group,[24] the present strategy of introducing the tribromoethenyl groups indeed improved the efficiency of demetallization of organometallic intermediates with a yield of over 90%. Additionally, we conducted DFT calculations on HsGDY in the gas phase and adsorbed on Au(111). Theoretical freestanding HsGDY networks with 1.65 nm (Supporting Information Figure S2a) primitive cell dimensions correspond well with the experimental measurement (1.65 ± 0.01 nm). The calculated HsGDY network structure on Au(111) and the corresponding STM simulation are also shown in Supporting Information Figure S2b,c. We also tried to deposit TTBEB molecules on Ag(111), and demetallization from organometallic intermediates was not achieved. The organometallic network on Ag(111) is shown in Supporting Information Figure S3.

We then tried to experimentally investigate the electronic structure of the HsGDY by using scanning
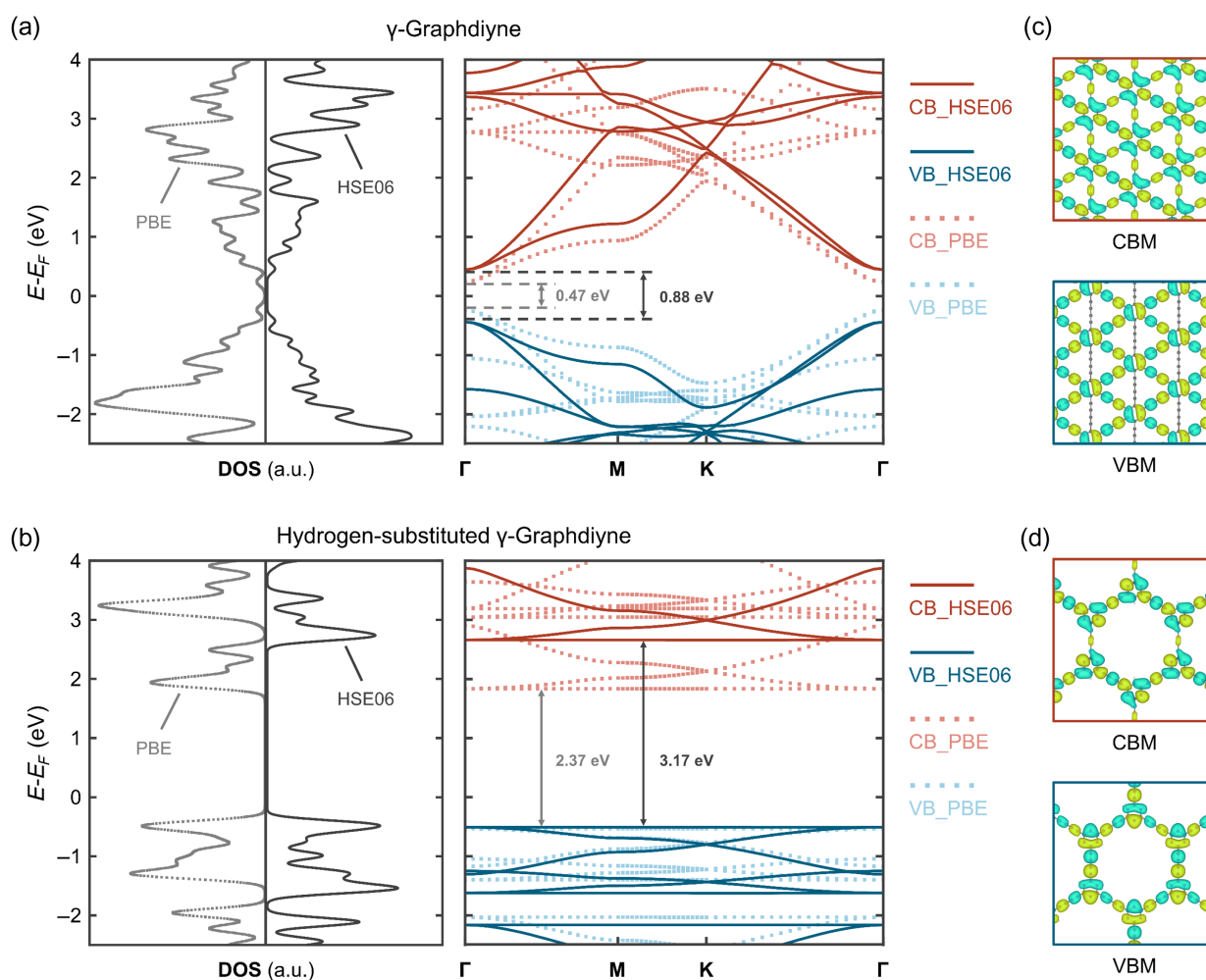

Figure 4 | *Theoretical electronic structure characterization of HsGDY. (a, b) Calculated DOS and band structures of the freestanding GDY and HsGDY from PBE (scatter plots) and HSE06 (line plots). (c, d) The LDOS distributions of the CBM and the VBM in GDY and HsGDY.*
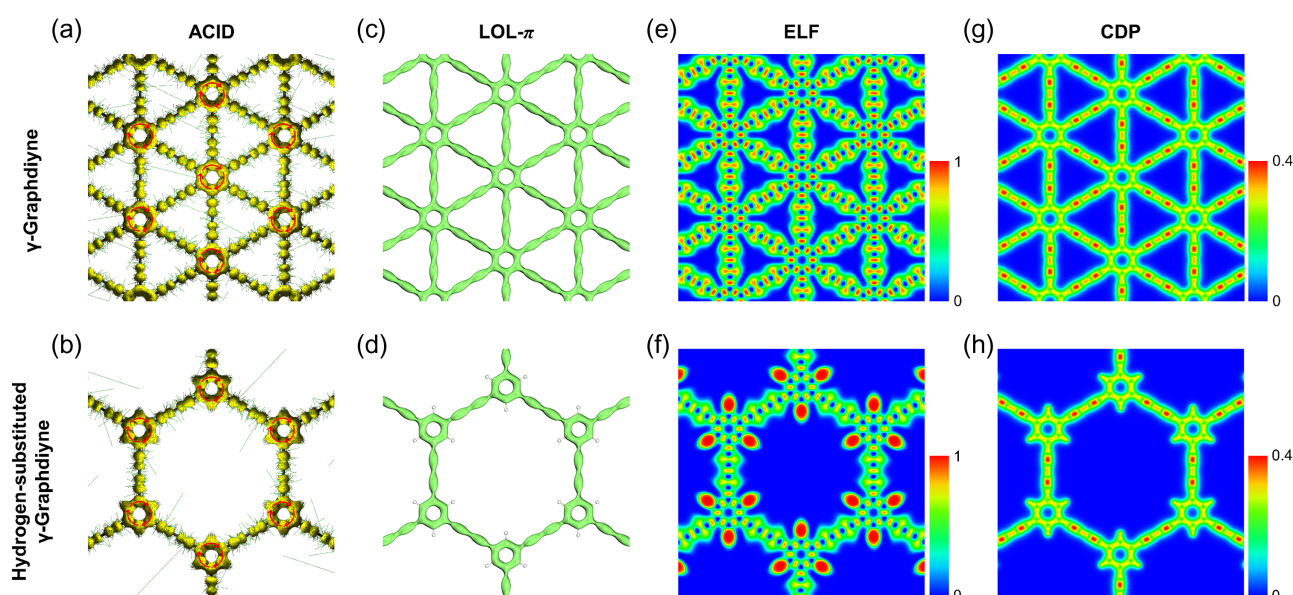
Figure 5 | *Calculated electronic properties of HsGDY. (a, b) Calculated ACID plots of GDY and HsGDY fragments (isovalue = 0.05, the red arrows indicate the ring current flow). (c, d) Isosurfaces of LOL-π of GDY and HsGDY fragments (isovalue = 0.40). (e, f) Calculated ELF of GDY and HsGDY. The scale of color bars is given in a.u. (g, h) Calculated CDP of GDY and HsGDY. The scale of color bars is given in e/Bohr³.*

tunneling spectroscopy. However, this was very challenging due to the large amount of surrounding bromine atoms. Therefore, we performed theoretical calculations to unveil the electronic characteristics of the HsGDY and compared the results with those of GDY. Scatter plots in Figure 4a,b show the calculated density of states (DOS) and band structures of freestanding GDY and HsGDY by the Perdew–Burke–Ernzerhof (PBE) exchange-correlation functional,[32] respectively. The direct bandgap in GDY was discovered to be 0.47 eV at Γ point, which is identical to the value previously anticipated,[9,33] and the larger gap value of 2.37 eV was theoretically obtained in HsGDY. Considering that the bandgaps are usually underestimated by PBE, we also performed calculations using the Heyd–Scuseria–Ernzerhof hybrid functional HSE06.[34] Indeed, the calculated band structures using HSE06 clearly displayed the wider bandgaps of 0.88 and 3.17 eV in GDY and HsGDY, respectively, as shown by line plots in Figure 4a,b. Another salient feature of the HsGDY band structure was the flat conduction band minimum (CBM) and valence band maximum (VBM), which was very similar to the halogen-substituted GDY[35] and hydrogen-substituted γ-graphyne.[36] Figure 4c,d also displays the local density of states (LDOS) distributions. We can see that, in diacetylene regions, the CBM was more localized at the carbon–carbon single bond sites, while the VBM was more localized at carbon–carbon triple bond sites, both in GDY and HsGDY.

To further gain additional insight into the electronic properties of HsGDY, anisotropy of the induced current density (ACID), localized orbital locator based on π

molecular orbitals (LOL-π), electron localization function (ELF), and charge density plot (CDP) calculations of HsGDY or its fragments were also conducted. They were compared with those in GDY. The estimated ACID plots (Figure 5a and Supporting Information Figure S4a for GDY fragment, Figure 5b and Supporting Information Figure S4b for HsGDY fragment) revealed that the 18-membered rings in GDY have a very weak aromatic character and that there is almost no visible ring current along their length. In both GDY and HsGDY, all benzene rings showed clockwise ring current flow, demonstrating their strong aromatic nature. The LOL-π calculations (Figure 5c and Supporting Information Figure S4c for GDY fragment, Figure 5d and Supporting Information Figure S4d for HsGDY fragment) showed that π electrons, notably in GDY, have favorable global conjugation channels. The electron conjugation over carbon–carbon triple bonds was more pronounced than that surrounding carbon–carbon single bonds, indicating the hindered conjugation over the π region of carbon–carbon single bonds.[37] According to the results of the ELF and CDP (Figure 5e,g for GDY, Figure 5f,h for HsGDY), we can infer that, in both structures, the electrons were delocalized, the carbon–carbon triple bonds were electron rich, and the benzene rings were comparatively electron poor.

Conclusions

In conclusion, we have demonstrated the feasibility of the construction of diacetylene moieties by on-surface reactions of precursors with tribromoethenyl groups,

showing higher efficiency than molecules with bromoalkynyl groups. Using such a strategy, single-layered HsGDY networks have been successfully synthesized, the fine structure of which has been characterized by STM and AFM, and HsGDY's electronic structure and properties have been studied by DFT calculations. This work may further inspire both theoretical and, especially, experimental work toward more delicate two-dimensional carbon nanostructures containing sp-hybridized carbon atoms.

Supporting Information

Supporting Information is available and includes the following information: materials and methods for STM/AFM measurements and DFT calculations; STM image of organometallic intermediate network on Au(111); DFT calculated models of freestanding HsGDY and HsGDY adsorbed on the Au(111) surface and simulated STM image of a HsGDY; STM images of the organometallic network on Ag(111); and a complete view of calculated ACID plots and isosurfaces of LOL-π of GDY and HsGDY fragments. (PDF)

Conflict of Interest

The authors declare no competing financial interest.

Acknowledgments

References

1. Krätschmer, W.; Lamb, L. D.; Fostiropoulos, K.; Huffman, D. R. Solid C_{60}: A New Form of Carbon. *Nature* **1990**, *347*, 354–358.
2. Iijima, S.; Ichihashi, T. Single-Shell Carbon Nanotubes of 1-nm Diameter. *Nature* **1993**, *363*, 603–605.
3. Novoselov, K. S.; Geim, A. K.; Morozov, S. V.; Jiang, D.; Zhang, Y.; Dubonos, S. V.; Grigorieva, I. V.; Firsov, A. A. Electric Field Effect in Atomically Thin Carbon Films. *Science* **2004**, *306*, 666–669.
4. Baughman, R. H.; Eckhardt, H.; Kertesz, M. Structure-Property Predictions for New Planar Forms of Carbon: Layered Phases Containing sp^2 and sp Atoms. *J. Chem. Phys.* **1987**, *87*, 6687–6699.
5. Kim, B. G.; Choi, H. J. Graphyne: Hexagonal Network of Carbon with Versatile Dirac Cones. *Phys. Rev. B* **2012**, *86*, 115435.

6. Li, Y.; Xu, L.; Liu, H.; Li, Y. Graphdiyne and Graphyne: From Theoretical Predictions to Practical Construction. *Chem. Soc. Rev.* **2014**, *43*, 2572–2586.
7. Kang, J.; Wei, Z.; Li, J. Graphyne and Its Family: Recent Theoretical Advances. *ACS Appl. Mater. Interfaces* **2019**, *11*, 2692–2706.
8. Li, G.; Li, Y.; Liu, H.; Guo, Y.; Li, Y.; Zhu, D. Architecture of Graphdiyne Nanoscale Films. *Chem. Commun.* **2010**, *46*, 3256–3258.
9. Long, M.; Tang, L.; Wang, D.; Li, Y.; Shuai, Z. Electronic Structure and Carrier Mobility in Graphdiyne Sheet and Nanoribbons: Theoretical Predictions. *ACS Nano* **2011**, *5*, 2593–2600.
10. Jiao, Y.; Du, A.; Hankel, M.; Zhu, Z.; Rudolph, V.; Smith, S. C. Graphdiyne: A Versatile Nanomaterial for Electronics and Hydrogen Purification. *Chem. Commun.* **2011**, *47*, 11843–11845.
11. Zhou, J.; Gao, X.; Liu, R.; Xie, Z.; Yang, J.; Zhang, S.; Zhang, G.; Liu, H.; Li, Y.; Zhang, J.; Liu, Z. Synthesis of Graphdiyne Nanowalls Using Acetylenic Coupling Reaction. *J. Am. Chem. Soc.* **2015**, *137*, 7596–7599.
12. Matsuoka, R.; Sakamoto, R.; Hoshiko, K.; Sasaki, S.; Masunaga, H.; Nagashio, K.; Nishihara, H. Crystalline Graphdiyne Nanosheets Produced at a Gas/Liquid or Liquid/Liquid Interface. *J. Am. Chem. Soc.* **2017**, *139*, 3145–3152.
13. Qian, X.; Liu, H.; Huang, C.; Chen, S.; Zhang, L.; Li, Y.; Wang, J.; Li, Y. Self-Catalyzed Growth of Large-Area Nanofilms of Two-Dimensional Carbon. *Sci. Rep.* **2015**, *5*, 7756.
14. Liu, R.; Gao, X.; Zhou, J.; Xu, H.; Li, Z.; Zhang, S.; Xie, Z.; Zhang, J.; Liu, Z. Chemical Vapor Deposition Growth of Linked Carbon Monolayers with Acetylenic Scaffoldings on Silver Foil. *Adv. Mater.* **2017**, *29*, 1604665.
15. He, F.; Li, Y. Advances on Theory and Experiments of the Energy Applications in Graphdiyne. *CCS Chem.* **2022**, *5*, 72–94.
16. Gao, X.; Liu, H.; Wang, D.; Zhang, J. Graphdiyne: Synthesis, Properties, and Applications. *Chem. Soc. Rev.* **2019**, *48*, 908–936.
17. Zheng, X.; Gao, X.; Vila, R. A.; Jiang, Y.; Wang, J.; Xu, R.; Zhang, R.; Xiao, X.; Zhang, P.; Greenburg, L. C.; Yang, Y.; Xin, H. L.; Zheng, X.; Cui, Y. Hydrogen-Substituted Graphdiyne-Assisted Ultrafast Sparking Synthesis of Metastable Nanomaterials. *Nat. Nanotechnol.* **2023**, *18*, 153–159.
18. Grill, L.; Dyer, M.; Lafferentz, L.; Persson, M.; Peters, M. V.; Hecht, S. Nano-Architectures by Covalent Assembly of Molecular Building Blocks. *Nat. Nanotechnol.* **2007**, *2*, 687–691.
19. Sun, Q.; Tran, B. V.; Cai, L.; Ma, H.; Yu, X.; Yuan, C.; Stohr, M.; Xu, W. On-Surface Formation of Cumulene by Dehalogenative Homocoupling of Alkenyl Gem-Dibromides. *Angew. Chem. Int. Ed.* **2017**, *56*, 12165–12169.
20. Cirera, B.; Sanchez-Grande, A.; de la Torre, B.; Santos, J.; Edalatmanesh, S.; Rodriguez-Sanchez, E.; Lauwaet, K.; Mallada, B.; Zboril, R.; Miranda, R.; Groning, O.; Jelinek, P.; Martin, N.; Ecija, D. Tailoring Topological Order and Pi-Conjugation to Engineer Quasi-Metallic Polymers. *Nat. Nanotechnol.* **2020**, *15*, 437–443.
21. Shu, C. H.; Liu, M. X.; Zha, Z. Q.; Pan, J. L.; Zhang, S. Z.; Xie, Y. L.; Chen, J. L.; Yuan, D. W.; Qiu, X. H.; Liu, P. N.

On-Surface Synthesis of Poly(p-Phenylene Ethynylene) Molecular Wires via in Situ Formation of Carbon-Carbon Triple Bond. *Nat. Commun.* **2018**, *9*, 2322.

22. Urgel, J. I.; Di Giovannantonio, M.; Eimre, K.; Lohr, T. G.; Liu, J.; Mishra, S.; Sun, Q.; Kinikar, A.; Widmer, R.; Stolz, S.; Bommert, M.; Berger, R.; Ruffieux, P.; Pignedoli, C. A.; Mullen, K.; Feng, X.; Fasel, R. On-Surface Synthesis of Cumulene-Containing Polymers via Two-Step Dehalogenative Homocoupling of Dibromomethylene-Functionalized Tribenzoazulene. *Angew. Chem. Int. Ed.* **2020**, *59*, 13281–13287.

23. Sun, Q.; Yu, X.; Bao, M.; Liu, M.; Pan, J.; Zha, Z.; Cai, L.; Ma, H.; Yuan, C.; Qiu, X.; Xu, W. Direct Formation of C–C Triple-Bonded Structural Motifs by On-Surface Dehalogenative Homocouplings of Tribromomethyl-Substituted Arenes. *Angew. Chem. Int. Ed.* **2018**, *57*, 4035–4038.

24. Sun, Q.; Cai, L.; Ma, H.; Yuan, C.; Xu, W. Dehalogenative Homocoupling of Terminal Alkynyl Bromides on Au(111): Incorporation of Acetylenic Scaffolding into Surface Nanostructures. *ACS Nano* **2016**, *10*, 7023–7030.

25. Liu, M.; Li, S.; Zhou, J.; Zha, Z.; Pan, J.; Li, X.; Zhang, J.; Liu, Z.; Li, Y.; Qiu, X. High-Yield Formation of Graphdiyne Macrocycles through On-Surface Assembling and Coupling Reaction. *ACS Nano* **2018**, *12*, 12612–12618.

26. Li, X.; Ge, H.; Gao, Y.; Yang, F.; Kang, F.; Xue, R.; Yan, L.; Du, S.; Xu, W.; Zhang, H.; Chi, L. Scanning Tunneling Spectroscopy Investigation of Au-bis-Acetylide Networks on Au (111): The Influence of Metal–Organic Hybridization. *J. Phys. Chem. Lett.* **2024**, *15*, 4593–4601.

27. Shu, C. H.; He, Y.; Zhang, R. X.; Chen, J. L.; Wang, A.; Liu, P. N. Atomic-Scale Visualization of Stepwise Growth Mechanism of Metal-Alkynyl Networks on Surfaces. *J. Am. Chem. Soc.* **2020**, *142*, 16579–16586.

28. Sanchez-Grande, A.; de la Torre, B.; Santos, J.; Cirera, B.; Lauwaet, K.; Chutora, T.; Edalatmanesh, S.; Mutombo, P.; Rosen, J.; Zboril, R.; Miranda, R.; Bjork, J.; Jelinek, P.; Martin, N.; Ecija, D. On-Surface Synthesis of Ethynylene-Bridged Anthracene Polymers. *Angew. Chem. Int. Ed.* **2019**, *58*, 6559–6563.

29. Riss, A.; Paz, A. P.; Wickenburg, S.; Tsai, H.-Z.; De Oteyza, D. G.; Bradley, A. J.; Ugeda, M. M.; Gorman, P.; Jung, H. S.; Crommie, M. F.; Rubio, A.; Fischer, F. R. Imaging Single-Molecule Reaction Intermediates Stabilized by Surface Dissipation and Entropy. *Nat. Chem.* **2016**, *8*, 678–683.

30. Kaiser, K.; Scriven, L. M.; Schulz, F.; Gawel, P.; Gross, L.; Anderson, H. L. An Sp-Hybridized Molecular Carbon Allotrope, Cyclo[18]Carbon. *Science* **2019**, *365*, 1299–1301.

31. Albrecht, F.; Rey, D.; Fatayer, S.; Schulz, F.; Perez, D.; Pena, D.; Gross, L. Intramolecular Coupling of Terminal Alkynes by Atom Manipulation. *Angew. Chem. Int. Ed.* **2020**, *59*, 22989–22993.

32. Perdew, J. P.; Burke, K.; Ernzerhof, M. Generalized Gradient Approximation Made Simple. *Phys. Rev. Lett.* **1996**, *77*, 3865–3868.

33. Srinivasu, K.; Ghosh, S. K. Graphyne and Graphdiyne: Promising Materials for Nanoelectronics and Energy Storage Applications. *J. Phys. Chem. C* **2012**, *116*, 5951–5956.

34. Paier, J.; Marsman, M.; Hummer, K.; Kresse, G.; Gerber, I. C.; Ángyán, J. G. Screened Hybrid Density Functionals Applied to Solids. *J. Chem. Phys.* **2006**, *124*, 154709.

35. Feng, Z.; Li, Y.; Tang, Y.; Chen, W.; Li, R.; Ma, Y.; Dai, X. Two-Dimensional Halogen-Substituted Graphdiyne: First-Principles Investigation of Mechanical, Electronic, Optical, and Photocatalytic Properties. *J. Mater. Sci.* **2020**, *55*, 8220–8230.

36. Kong, X.; Li, L.; Peeters, F. M. Graphene-Based Heterostructures with Moiré Superlattice That Preserve the Dirac Cone: A First-Principles Study. *J. Phys. Condens. Mat.* **2019**, *31*, 255302.

37. Lu, T.; Chen, Q. A Simple Method of Identifying π Orbitals for Non-Planar Systems and a Protocol of Studying π Electronic Structure. *Theor. Chem. Acc.* **2020**, *139*, 25.